UCLA/PPG--980

DE86 010867

MATERIALS EROSION AND REDEPOSITION STUDIES AT THE PISCES FACILITY -NET EROSION UNDER REDEPOSITION-

Y. Hirooka, D.M. Goebel, R.W. Conn, W.K. Leung
and G.A. Campbell

May, 1986

UCLA/PPG-980

DISCLAIMER

Department of Mechanical, Aerospace
and Nuclear Engineering
Center for Plasma Physics and Fusion Engineering
University of California, Los Angeles
Los Angeles, California 90024, USA

Paper presented at 2nd International Conference on Fusion Reactor Materials
at Chicago, 1986 (to be published in J. Nucl. Mater.)

MATERIALS EROSION AND REDEPOSITION STUDIES AT THE PISCES FACILITY -NET EROSION UNDER REDEPOSITION-

Y. Hirooka, D.M. Goebel, R.W. Conn, W.K. Leung and G.A. Campbell

Department of Mechanical, Aerospace and Nuclear Engineering
Center for Plasma Physics and Fusion Engineering
University of California, Los Angeles
Los Angeles, California 90024, USA

Abstract

Simultaneous erosion and redeposition of copper and 304 stainless steel under controlled and continuous plasma (D,He,Ar) bombardment has been investigated in the PISCES-facility, which generates typical edge-plasma conditions of magnetic fusion devices. The plasma bombardment conditions are: incident ion flux in the range from 10^{17} to 10^{18} ions/sec/cm^2, ion bombarding energy of 100 eV, electron temperature in the range from 5 to 15 eV, plasma density in the range from 10^{11}-10^{13} cm^{-3}, target temperature in the range from 300 to 900K, and the total ion fluence in the range from 10^{20} to 10^{22} ions/cm^2. The net erosion yield under redeposition is found to be significantly smaller than the classical sputtering yield data. A first-order modeling is attempted to interpret the erosion and redeposition behavior of materials under plasma bombardment. It is pointed out both theoretically and experimentally that the mean free path for electron impact ionization of the sputtered material is the key parameter to control the overall mechanism of erosion and redeposition. Strongly modified surface morphologies of bombarded targets are observed and indicate a retrapping effect.

Key Words: Coatings (surface modification, redeposited materials, sputtering), Copper, First wall (copper alloy), Models (erosion and redeposition), Sputtering (redeposition of materials), Stainless steel, Surface Analysis, Surface damage, PISCES

1. Introduction

Over the last two decades, the fusion reactor materials community has made a considerable effort to evaluate first wall component erosion due to sputtering [1-4]. On the other hand, it is theoretically understood that redeposition associated with reionization and transport of sputtered particles in a magnetically confined plasma can significantly affect the erosion behavior of surface components such as limiter and divertor plates [5]. However, the redeposition behavior of materials has not been experimentally studied since it is generally difficult to control key parameters of the plasma in contact with these surface components of a toroidal fusion device operating in short pulse modes.

In the present work, the PISCES-facility [6,7] is used to carry out controlled and continuous plasma bombardment under typical edge-plasma simulated conditions. These conditions are such that sputtered particles are ionized by electron impact within a magnetized plasma, trapped on the magnetic field lines and redeposited back on the original surface. To the best of our knowledge, this paper presents the first experimental results and analysis of the net erosion yields of materials under simultaneous redeposition.

2. Experimental details

The PISCES-facility was previously described in detail elsewhere [6,7]. A schematic diagram of the present experimental arrangement is shown in Fig. 1. The magnetic field in the target region is typically 2.5×10^{-2} T, which constricts the plasma stream diameter to be approximately 10 cm. A mechanically polished sample with a diameter of 2.5 cm was placed on a target holder with either water or air cooling. The sample is well within the homogeneous density region of the plasma [6,7]. A Langmuir probe was positioned in front of the target surface to measure the electron temperature and plasma density. The electron temperature and plasma density are typically in the ranges from 5 to 15 eV and 10^{11} to 10^{13} cm^{-3}, respectively.

Since the ion temperature for the plasma generated in the PISCES facility is usually a few electron volts [8], the actual ion bombardment energy is controlled by applying a negative bias to the target in addition to the floating potential, which is $\sim 3kT_e$ with respect to the plasma. The total negative potential at the target was set at 100 V in the present study. The thickness of the sheath generated by the negative potential is a few tens of microns under the present plasma operation conditions. Because of the sheath acceleration, ions are considered to impinge on the target at normal incidence, regardless of their prior ion-gyration direction.

The ion flux was in the range from 5×10^{17} to 5×10^{18} ions/sec/cm^2. This means that the target is subject to a heat flux up to about 80 W/cm^2 after applying a negative bias. The target temperature was controlled to be between 300 to 900 K by either air or water cooling. The total ion fluence was varied between 10^{20} and 10^{22} ions/cm^2.

3. Results and discussion

3-1. First-order modeling of erosion and redeposition behavior of materials in PISCES

A simple modeling is attempted here to analyze the erosion and redeposition behavior of materials, particularly in the PISCES-facility, although more elaborate computer programs are being developed (e.g., REDEP [9]) for toroidal confinement devices. The important processes involved in this model are: (1) the incident ions impinge on the target surface with the energy given by the total sheath potential and cause sputtering; (2) sputtered atoms are ionized by electron impact within the plasma stream if the mean free path for the ionization process is moderately short for a given electron temperature and density; (3) the reionized particles are trapped on linear magnetic field lines and transported back to the target due to a pre-sheath electric field (approximately $-1.5kT_e$ for the PISCES-facility [9]); (4) these redepositing ions impinge on the surface being accelerated by the sheath potential and then cause self-sputtering; and (5) the self-sputtered particles will repeat the same processes as those described in (2), (3), and (4).

The sputtering yield, Y_s, for the primary plasma ion-target combination and the self-sputtering yield, Y_{ss}, due to redepositing ions are estimated by Yamamura's analytical formula [3]:

$$Y_s = 0.42 \frac{\alpha^* QKS_n(\varepsilon)}{U_s\{1 + 0.35U_sS_e(\varepsilon)\}} \{1 - (E_{th}/E_i)^{0.5}\}^{2.8} \quad . \qquad (1)$$

The terms α^* and Q are empirical parameters; E_{th} is the threshold energy for sputtering; K is the conversion factor from the elastic reduced stopping cross section to the stopping cross section; $S_n(\varepsilon)$ and $S_e(\varepsilon)$ are Linhard's elastic and inelastic reduced stopping cross section, respectively; U_s is the surface binding energy; E_i is the energy of the incident ion. Calculated sputtering yields for the selected ion-target combinations are shown in Table 1. Unless otherwise specified, only physical sputtering is treated for simplicity. It is reasonable to assume sputtered atoms to be 100% neutral since normally the secondary positive and/or negative ion formation rates due to ion bombardment are negligibly small, except for alkaline metals [10].

Unless reliable experimental data is available, the cross section for electron impact ionization of the target material, σ, is calculated from Lotz's formula [11]:

$$\sigma = \sum_{i=1}^{N} a_i q_i \frac{\ln(E_e/P_i)}{E_e P_i} [1 - b_i \exp\{-c_i(E_e/P_i - 1)\}] \quad . \tag{2}$$

E_e is the energy of the impact electron; P_i is the binding energy of electrons in the i-th subshell: q_i is the number of equivalent electrons in the i-th subshell; a_i, b_i and c_i are fitting parameters. The cross section is averaged over the Maxwellian energy distribution in order to determine the ionization rate coefficient, $\langle\sigma v\rangle$. The mean free path for electron impact ionization, λ, is given by:

$$\lambda = \frac{\bar{V}}{n_e \langle\sigma V\rangle} \quad , \tag{3}$$

where n_e is the electron density. The term, $\bar{V}$, is the averaged velocity of sputtered particles over the energy distribution [1]:

$$N(E) = \frac{E}{(E + U_s)^3} \quad , \tag{4}$$

where E is the energy of the sputtered particle. The tail of the energy distribution exceeding the pre-sheath potential is cut off before averaging. However, this cut-off effect on the resultant average velocity is as small as 5~10%. The result of the mean free path evaluation by Eqs. (2), (3) and (4) will be shown later.

The probability of redeposition is defined as the fraction of sputtered particles which will be ionized within the projected space of the target surface area along the major machine axis (see Fig. 1). Assuming that the emission of sputtered neutrals obeys the cosine law, the flux of sputtered neutrals, J, arriving at an area dA at (x,θ), is given by the following equation [12]:

$$J(x,\theta) = I_o Y_s \left(\frac{R}{x}\right)^2 / (1 + \tan^2\theta)^2 \quad , \tag{5}$$

where R is the radius of the target and I_o is the bombarding ion flux. The fraction of ionized atoms at a distance, y, from the origin is given by the relation [13]:

$$f(y) = 1 - \exp(-y/\lambda) \quad . \tag{6}$$

Substituting $x=R/\tan\theta$ and $y=R/\sin\theta$ into Eqs. (5) and (6), the probability of redeposition can be expressed as a function of λ:

$$P(\lambda) = \frac{\int_0^{\pi/2} f(\theta)\, J(\theta) d\theta}{\int_0^{\pi/2} J(\theta) d\theta} \quad . \tag{7}$$

As shown in Fig. 2, the probability of redeposition, $P(\lambda)$, decreases rapidly as λ increases.

Calculated mean free paths for electron impact ionization of physically sputtered copper, as an example, are shown in Fig. 3. Notice that the second and third ionization mean free paths are appreciably large compared with the first one. Knowing the nature of $P(\lambda)$ shown in Fig. 2, multi-charged ions are considered to have little possibility of redeposition in the present experiment. Therefore, we assume that singly charged ions are the only species of redepositing particles. This means that these redepositing ions are considered to bombard the target with the same energy as that for the primary plasma ions.

Using the probability of redeposition, the net erosion rate, dw/dt, is given by

$$dw/dt = I_o Y_s \{1 - P(\lambda)\} [1 + \{Y_{ss} - (1 - R_e)\} \sum_{k=1}^{\infty} \{Y_{ss} P(\lambda)\}^k] , \quad (8)$$

where R_e is the particle reflection coefficient, which is calculated by TRIM Monte-Carlo program [4] for redepositing ions. The term, $(1 - R_e)$, is equivalent to the trapping coefficient of redepositing ions. The first term of the infinite series is due to the primary plasma ions, and the second term is due to the first generation of redepositing ions. The succeeding terms are explained likewise.

Note that when the probability of redeposition is negligibly small, the net erosion rate estimated by Eq. (8) becomes essentially the same as the sputter erosion due to the primary plasma ions. This means that if λ is large, most of the sputtered particles escape from the plasma as neutrals in which case the plasma stream acts virtually as an ion beam. As such, the ionization mean free path for sputtered atoms is the key parameter governing the overall erosion and redeposition behavior of materials in the present work. Also, if Y_{ss} is smaller than the trapping coefficient, the resultant net erosion rate will be smaller than the classical sputtering erosion rate. Another important implication of Eq. (8) is that the "run-away erosion" criterion for the PISCES-facility is: $Y_{ss}P(\lambda) > 1$, which is similar to that for large toroidal confinement devices [5].

3-2. Experimental data and analysis

A summary of representative experimental data is shown in Table 1. Notice that the "run-away erosion" condition is avoided in the present work. The normalized erosion yield, Y_n, is defined as:

$$Y_n \equiv \frac{\Delta W_m}{\Delta W_t} \quad , \tag{9}$$

where ΔW_m is the measured weight loss of a target after plasma bombardment, and ΔW_t is the theoretical weight loss estimated from the sputtering yield. The normalized erosion yields are plotted as a function of mean free path, λ_1, for the first ionization of sputtered atoms in Fig. 4. The normalized erosion yield becomes significantly smaller than unity when λ_1 is smaller than about 10 cm (referred to as the "Redeposition-dominated regime" in Fig. 4). This means that the net erosion rate under redeposition is reduced relative to the classical sputter erosion rate. As λ_1 increases, the net erosion rate approaches the sputter erosion rate ("Erosion-dominated regime").

The first-order theory is compared with the normalized erosion yield data in Fig. 4. There is generally agreement between the theory and experimental data. However, the theory appears to overestimate the erosion yield, particularly in the redeposition-dominated regime. Importantly, there is a tendency that redeposited materials with strongly modified surface morphologies (see Fig. 5b) represent data points with large negative deviations whereas those with relatively smooth surface morphologies (see Fig. 5c) show good agreement with the theory. This indicates that the strongly modified surfaces such as those with dense cone structures may have some retrapping nature to reduce the sputtering yield [1,14], which results in the discrepancy between the theory and experimental data. The present theory needs to be improved in this regard [15]. Also, no major impurity was found on these redeposited surfaces by AES (Auger Electron Spectroscopy) analysis although a trace amount, less than a few atomic percent, of molybdenum was detected on the cone-covered surface by SIMS (Secondary Ion Mass Spectroscopy) analysis. The surface morphology might be affected by the presence of impurities during plasma bombardment. A detailed discussion of mechanisms driving the surface morphology evolution can be found elsewhere [15].

4. Conclusion

The first non-tokamak, controlled plasma-wall experiments have been carried out with the main objective of investigating the erosion behavior of materials under simultaneous redeposition conditions. In the redeposition-dominated regime, the net erosion yield is found to be considerably smaller than the classical sputtering yield. A simple theory has been developed and has characterized the net erosion and redeposition behavior of materials by the mean free path for electron impact ionization of the sputtered material. Strongly modified surfaces are observed for redeposited materials and imply some topographical retrapping effect which further reduces the erosion yield.

Acknowledgment

Illuminating discussions with K.L. Wilson (SNLL), W. Gauster(SNLL), A.R. Krauss (ANL) and J. Bohdansky (IPP) are sincerely appreciated. Technical assistance for experiments by T. Sketchley and V. Low and the computer data acquisition arrangement by K. Andrews are also acknowledged. This work is supported by the Office of Fusion Energy, U.S. Department of Energy Contract #DE-AT03-84ER52104.

References

[1] R. Behrish, "Sputtering by Particle Bombardment Vol. 1 & 2," Springer-Verlag Berlin Heidelberg (1981 & 1983).

[2] E.W. Thomas, ORNL-6088/Vol. 3, (Feb., 1985).

[3] N. Matsunami et al., Atom. Data and Nucl. Data Tables 31 (1984) 1.

[4] J. P. Biersack and L.G. Haggmark, Nucl. Instr. & Methods 174 (1980) 257.

[5] INTOR Report, Phase-2A, Part-1, IAEA, Chap. 7 (1983).

[6] D.M. Goebel, G. Campbell and R.W. Conn, J. Nucl. Mater. 121 (1984) 277.

[7] D.M. Goebel and R.W. Conn, J. Nucl. Mater. 128 & 129 (1984) 249.

[8] G. Tynan, MS Thesis at UCLA (1986).

[9] J.N. Brooks, J. Nucl. Mater. 111 & 112 (1982) 457.

[10] A.R. Krauss and D.M. Gruen, J. Nucl. Mater. 85 & 86 (1976) 1179.

[11] W. Lotz, Z. Physik 206 (1967) 205.

[12] E. Rutner, P. Goldfinger and J.I. Hirth, Condensation and Evaporation of Solids, Gordon and Breach Sci. Pub., Sec. -1 (1964).

[13] M.R. Wehr, J.A. Richards, Jr., T.W. Adair, III, Physics of the Atoms, 4th ed., Addison-Wesley, Chap. 1 (1984).

[14] O. Auciello and R. Kelly, Ion Bombardment Surface Modification, Elsevier (1984).

[15] Y. Hirooka, D.M. Goebel, R.W. Conn, G.A. Campbell, W.K. Leung, K.L. Wilson, R.A. Causey, D.H. Morse and J. Bohdansky, To be published in Nucl. Instr. & Meth.-B (Presented at International Workshop on Surface Modification by Plasma Bombardment at Princeton, May, 1986).

[16] R.H. Huddelstone and S.L. Leonard, Plasma Diagnostic Techniques, Academic Press, New York, Chap. 4 (1965).

Figure Captions

Fig. 1: A schematic diagram of the experimental setup.

Fig. 2: Probability of redeposition as a function of mean free path for electron impact ionization of sputtered atoms.

Fig. 3: Mean free paths for 1st, 2nd and 3rd ionization of physically sputtered copper. The electron density is obtained from the relation [16]: $I_o = 0.5 N_e \sqrt{(kT_e/m)}$ for a given flux and electron temperature. In this case, a typical Ar^+ ion flux of 1.0×10^{18} ions/cm^2sec is assumed.

Fig. 4: Comparison between experimental data and theoretical curves of normalized erosion yield as a function of mean free path of the 1st ionization.

Fig. 5: Surface morphologies of copper targets: (a) as-polished, (b) bombarded by Ar-plasma with the presence of molybdenum, and (c) bombarded by Ar-plasma without impurities. The total ion flunece is about 2×10^{21} ions/cm^2 for (b) and (c).

Table 1. Summary of representative data from the erosion and redeposition experiments.

Target Material	Target Temp. (K)	Plasma Species	I_o (ions/cm^2·sec)	Ion Fluence (ions/cm^2)	$Y_s(Y_{ss})^*$ (atoms/ion)	R_e^*	T_e (eV)	N_e (1/cm^3)	λ_i (cm)	ΔW_m (mg)	ΔW_t (mg)	Y_n
Cu	334	Ar^+	1.37×10^{18}	2.47×10^{21}	0.429(0.395)	0.197	9.6	5.6×10^{12}	1.78	135.	350.	0.384
Cu	343	Ar^+	5.7×10^{17}	2.1×10^{21}	0.429(0.395)	0.197	4.2	3.5×10^{12}	12.2	128.	284.	0.440
Cu	323	He^+	4.05×10^{17}	1.46×10^{21}	0.0543(0.395)	0.197	7.4	6.1×10^{11}	18.3	22.5	24.0	0.859
Cu	330	He^+	1.98×10^{17}	7.14×10^{20}	0.0543(0.395)	0.197	7.5	3.0×10^{11}	36.9	11.7	12.8	0.911
304SS	828	Ar^+	1.22×10^{18}	4.39×10^{21}	0.210(0.188)	0.213	13.2	4.3×10^{12}	1.23	37.8	270.	0.143
304SS	873	Ar^+	2.93×10^{17}	4.74×10^{21}	0.210(0.188)	0.213	6.4	1.5×10^{12}	9.56	13.5	29.1	0.465

* Calculated for the ion energy of 100 eV.

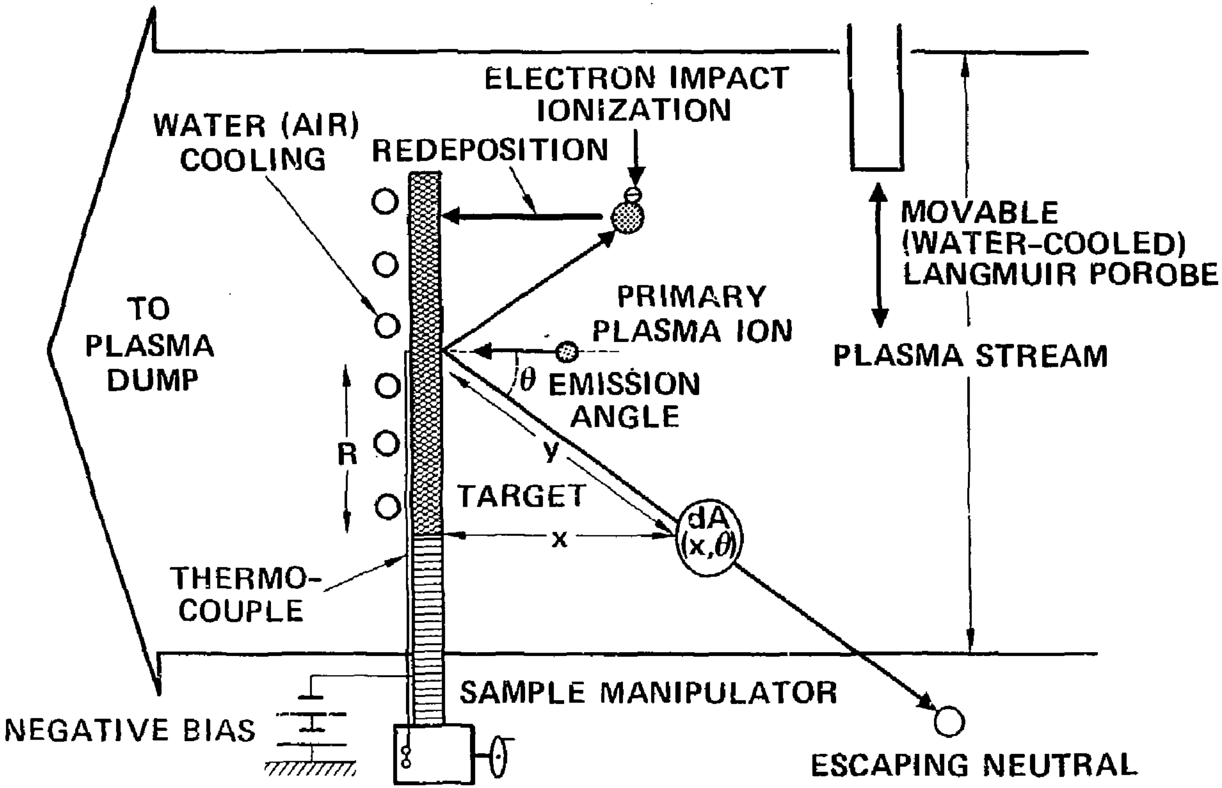

ELECTRON IMPACT
IONIZATION
WATER (AIR)
COOLING
REDEPOSITION
MOVABLE
(WATER-COOLED)
LANGMUIR POROBE
TO
PLASMA
DUMP
PRIMARY
PLASMA ION
PLASMA STREAM
θ EMISSION
ANGLE
R
y
TARGET
dA
(x,θ)
x
THERMO-
COUPLE
SAMPLE MANIPULATOR
NEGATIVE BIAS
ESCAPING NEUTRAL

FIGURE 1

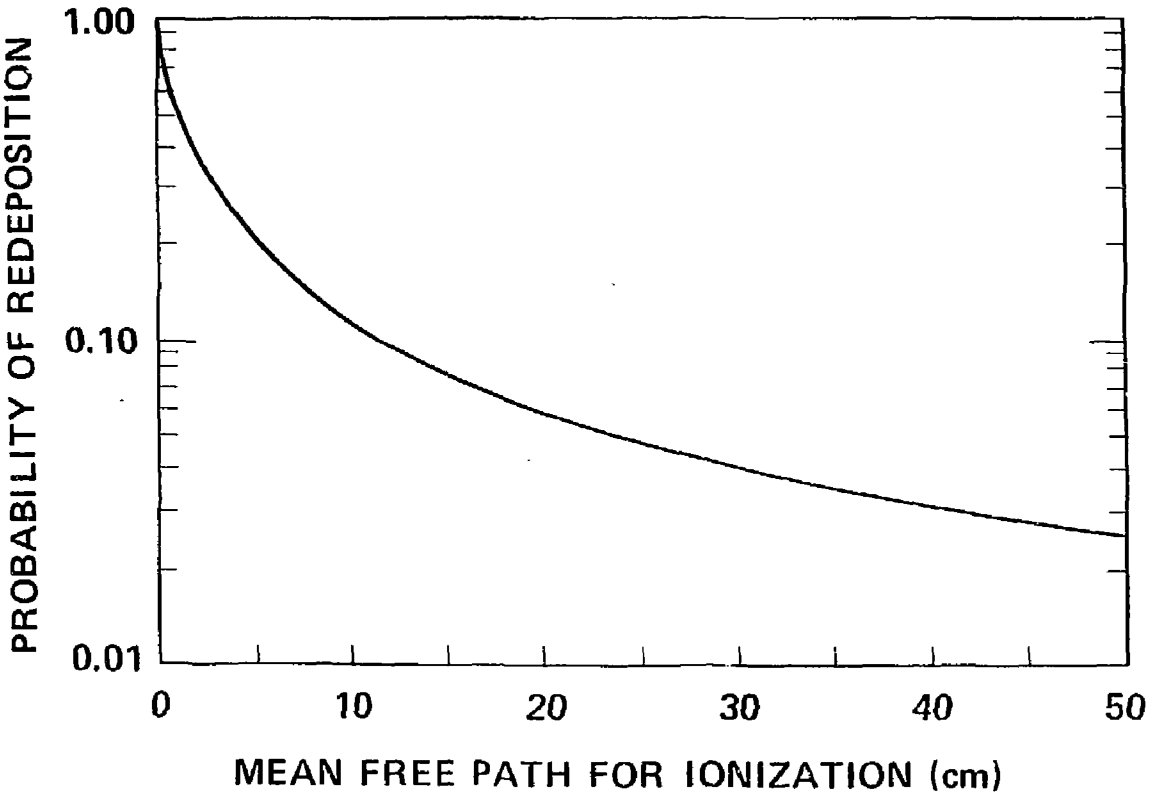
1.00
0.10
0.01
PROBABILITY OF REDEPOSITION
0
10
20
30
40
50
MEAN FREE PATH FOR IONIZATION (cm)

FIGURE 2

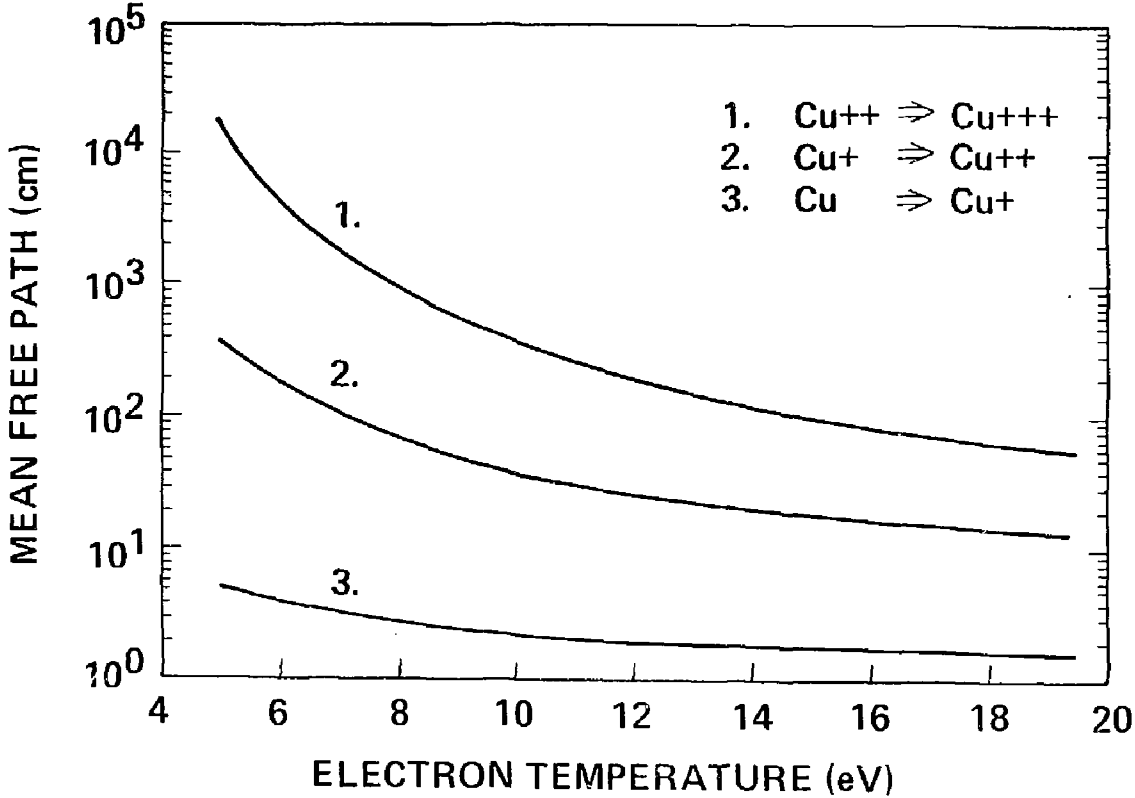
MEAN FREE PATH (cm)
ELECTRON TEMPERATURE (eV)
1. Cu++ ⇒ Cu+++
2. Cu+ ⇒ Cu++
3. Cu ⇒ Cu+
1.
2.
3.

FIGURE 3

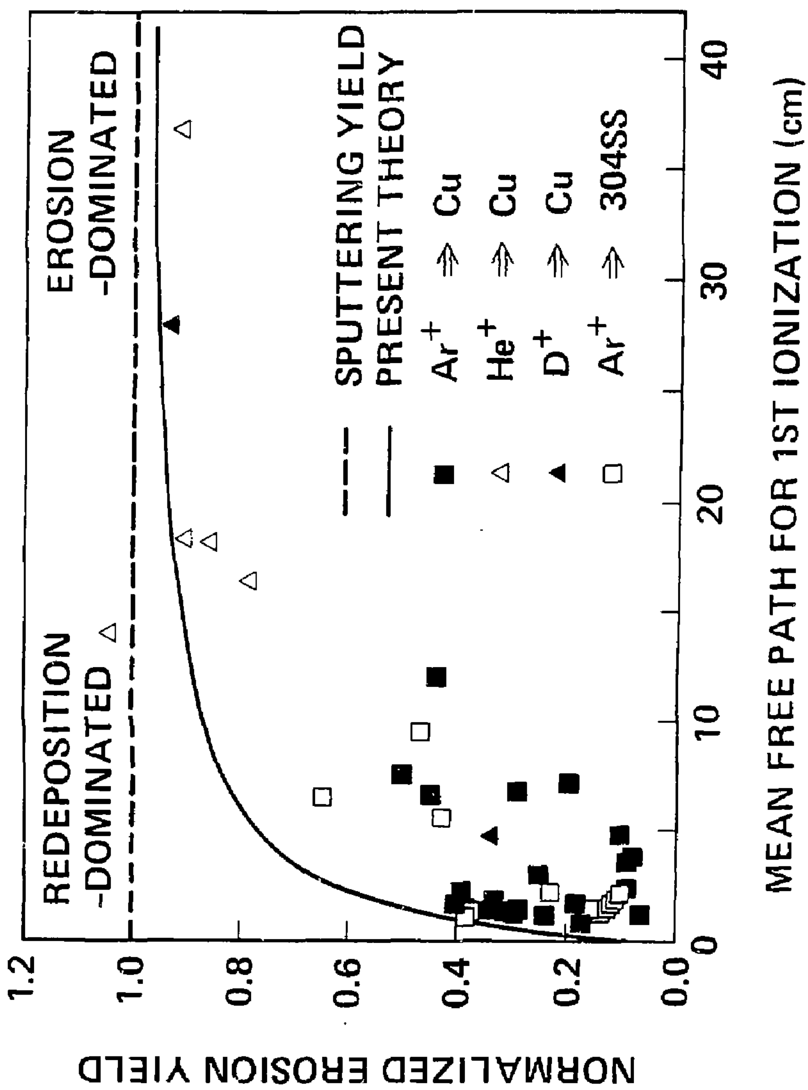
NORMALIZED EROSION YIELD
1.2
1.0
0.8
0.6
0.4
0.2
0.0
0
10
20
30
40
MEAN FREE PATH FOR 1ST IONIZATION (cm)
REDEPOSITION
-DOMINATED
EROSION
-DOMINATED
SPUTTERING YIELD
PRESENT THEORY
Ar+ → Cu
He+ → Cu
D+ → Cu
Ar+ → 304SS

FIGURE 4

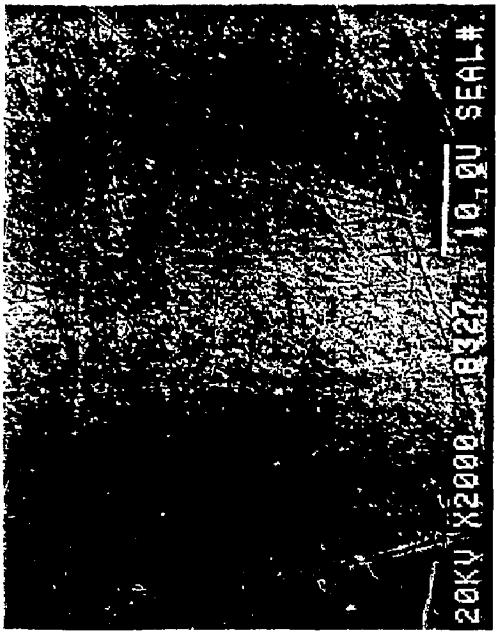

a

b

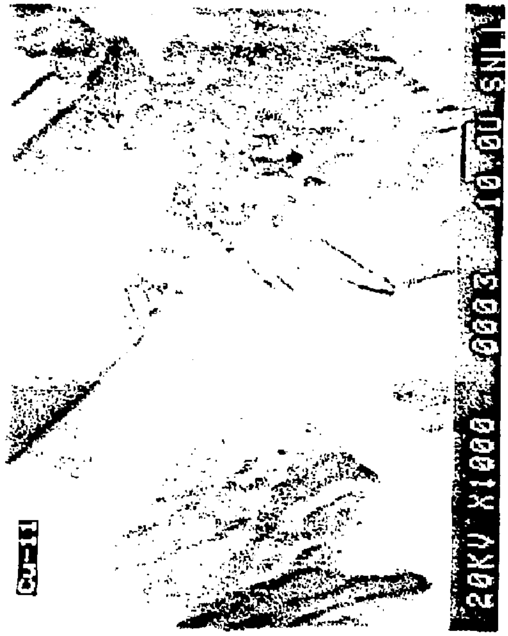

c

FIGURE 5